Precision Engineering 35 (2011) 51–57

Contents lists available at ScienceDirect

Precision Engineering

journal homepage: www.elsevier.com/locate/precision

Molecular dynamics simulation of the material removal mechanism in micro-EDM

Xiaodong Yang [a,*], Jianwen Guo [a], Xiaofei Chen [a], Masanori Kunieda [b]

[a] Department of Mechanical Engineering and Automation, Harbin Institute of Technology, Harbin 150001, China
[b] Department of Mechanical Systems Engineering, The University of Tokyo, Tokyo 113-8656, Japan

ARTICLE INFO

Article history:
Received 26 January 2010
Received in revised form 15 June 2010
Accepted 30 June 2010
Available online 9 September 2010

Keywords:
Micro-EDM
Discharge crater
Material removal
Molecular Dynamics (MD)
Computer simulation

ABSTRACT

Electrical discharge phenomena in EDM occur in a very short time period and in a very narrow space, thus making both observation and theoretical analysis extremely difficult. For this reason, the material removal mechanism in EDM has yet to be understood clearly. In this paper, the forming process of discharge craters in three dimensions was simulated, and material removal mechanism in EDM was analyzed using Molecular Dynamics (MD). It was found that material removal mechanism in EDM can be explained in two ways; one by vaporization and the other by the bubble explosion of superheated metals. It was also found that the metal removal efficiency is 0.02–0.05, leaving most of the melted pool resolidified. In addition, the influence of power density on the removal process was investigated, and the results showed that as the power density increases, the diameter and depth of the melted area increase, as does the metal removal efficiency. In this study, the forming mechanism of the bulge around discharge craters was also analyzed, and it was found that bulge is formed due to two mechanisms. The first is the shearing flow of the molten material caused by the extremely high pressure in the superheated material, and the second is the accumulation of the ejected material on the bulge formed by the first forming mechanism. It was also found that existence of micro pores in the workpiece material increases the depth of the discharge crater and melted area, thereby increasing the machining surface roughness. Simulation of the distribution of removed materials in the gap showed that some part of the removed material becomes debris ejected from the gap, while another part settles on the surface of the opposite electrode, and the last part returns to the surface of the electrode from which it was ejected.

1. Introduction

Electrical Discharge Machining (EDM) technology has developed rapidly and become indispensable in manufacturing applications such as die and mold making, micro-machining, prototyping, etc. However, EDM gap phenomena are very complicated and hence not yet fully understood. Understanding arc discharges continues to be a difficult problem, even in the steady state. Electrical discharge phenomena in EDM occur in a very short time period and in a very narrow space, thus making both observation and theoretical analysis extremely difficult.

EDM is a thermal process. Thermal energy generated by a pulse discharge between the workpiece and tool electrode results in melting and evaporation followed by material removal of both the workpiece and tool electrode, forming a crater on both surfaces. Since the EDM process is the repetition of this phenomenon caused by a single pulse discharge, research on the formation of discharge craters can help understand the material removal mechanism and improve the machining characteristics of EDM. For this reason, many studies have been conducted on discharge craters. For example, Yoshida et al. compared the discharge craters generated in air dielectric with those in liquid dielectric [1]. Araie et al. investigated the shape characteristics of craters in micro-EDM [2]. However, these researches only aimed at investigating the final shape of craters, and the material removal mechanism and the forming process of discharge craters have yet to be understood well. Since it is very difficult to clarify the electrical discharge phenomena in EDM experimentally, it is sometimes more useful to resort to simulation methods. Numerous attempts have been made to calculate temperature distribution in electrodes by solving time-dependent heat transfer equations based on various heat source models [3,4]. However, these heat transfer models cannot demonstrate the dynamics of material removal.

To investigate the forming process of discharge craters and explain the material removal mechanism from a microscopic view, the workpiece material should be taken to be an aggregation of

* Corresponding author at: Department of Mechanical Engineering and Automation, Harbin Institute of Technology, P.O. 421, 92 West DaZhi Street, Nangang District, Harbin 150001, China. Tel.: +86 451 86418084; fax: +86 451 86413485.
E-mail address: xdyang@hit.edu.cn (X. Yang).

0141-6359/$ – see front matter © 2010 Elsevier Inc. All rights reserved.
doi:10.1016/j.precisioneng.2010.09.005

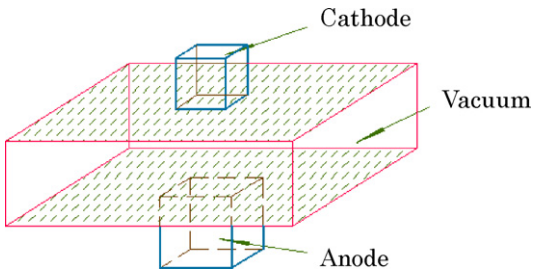

Fig. 1. Schematic diagram of model.

discrete particles. Molecular Dynamics (MD) simulation is a useful method to simultaneously analyze the mechanical and thermal behaviors of material in the atomic scale [5–7]. MD has therefore been widely used in the simulations of cutting and grinding processes in the nano-scale, and laser machining which is categorized as a thermal process like EDM. In recent years, applications of MD in electrical-machining have been reported by Kalyanasundaram et al. who studied the 'quasi-solid' behavior of the dielectric *n*-decane at the nano-EM interface [8], Shimada et al. who studied the mechanism of the self-sharpening phenomenon of thin tungsten electrodes in single discharge [9], and Cui who simulated the electrode deposition process using the MD method [10].

Thus, this study aimed to visualize the forming process of discharge craters in three dimensions with relatively small discharge energy and clarify the mechanism of material removal and formation of discharge crater shapes. Moreover, influences of micro defects like micro pore preexisting in the workpiece material prior to the occurrence of discharge on the forming process of craters were studied. In addition, the dynamic mass transfer of removed materials across the gap was also investigated.

2. MD modeling

2.1. Model and boundary conditions

There are three domains in the model as shown in Fig. 1: anode, cathode, and gap. The sizes of the anode and cathode are $60a \times 60a \times 32a$ and $53a \times 53a \times 19a$, where a indicates the crystal lattice constant, made up of 460,800 and 213,484 atoms, respectively. Both anode and cathode materials are copper, and discharge is ignited on the surface where the crystal orientation is {1 0 0}. The domain of the gap between the two electrodes is about 1200 Å × 1200 Å × 80 Å in size. Considering that in actual EDM processes, the working gap is mostly occupied by bubbles even though the working gap is submerged in dielectric liquid [11], the working gap is taken to be a vacuum for simplicity.

The initial MD model of the electrode: either anode or cathode, before electrical discharge is shown in Fig. 2. Fixed boundary conditions are applied to the electrode surfaces except the working surface where discharge is ignited, and the thickness of the fixed boundary layer is about $2.5a$. The atoms in the layer of $1.5a$ in thickness adjacent to the boundary atoms act as thermostat atoms. The

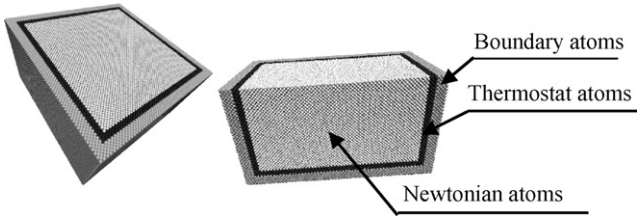

Fig. 2. Initial MD model of electrode.

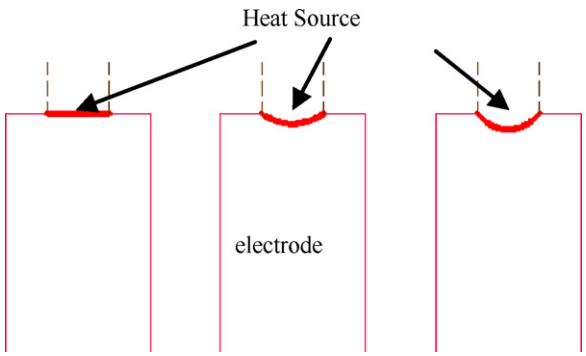

Fig. 3. Schematic diagram of shape-changing heat source.

other part of the electrode is the Newtonian layer where the atoms obey Newton's second law. Free boundary conditions are applied to the working surface. Through the free surface, thermal energy is input into the electrodes. With regards to the boundary conditions of the gap, for the horizontal surfaces parallel to the working surfaces of electrodes, areas contacting the electrodes are applied with free boundary conditions, and other areas are applied with the 'wall' boundary condition where colliding atoms are bounced. The four side surfaces are applied with free boundary conditions.

2.2. Heat source

In this model, a circular heat source acts on the free surface of both electrodes i.e. anode and cathode at the center to imitate the heat flux from the discharge column. It is assumed that the diameter of the heat source is equal to that of the arc column. The temperature in the discharge column is assumed to be constant at 7000 K based on spectroscopic measurement results [12]. However, the shape of the heat source is variable according to the moving boundary on the free surface of the electrode due to the formation of discharge craters. Schematic diagram of the shape-changing heat source is shown in Fig. 3.

To imitate the input of thermal energy, the velocity for each atom in the heat source is determined statistically so as to follow the Maxwell–Boltzman's distribution at the discharge column temperature. Power density can be changed by varying the area density of the number of atoms in the heat source where thermal energy is supplied to the atoms. The resultant power density can be calculated by dividing the difference in the total energy of the electrode before and after discharge with the area of the heat source. Due to the calculation capacity of the computer used, the time scale in MD is limited to within several tens of ps. In this extremely short time scale, the discharge column can be assumed to be stationary at the center of the electrode. For simplicity, in this study, the gap was assumed to be in vacuum before dielectric breakdown. The formation of the arc column was not dealt with, hence particles composing the arc column: ions, electrons, and neutral atoms, were ignored.

2.3. Interatomic potential

In this study, the embedded-atom method [13] was employed to express the interatomic potential in the copper structure. The total energy E_{tot} of an elemental system can be represented as

$$E_{tot} = \frac{1}{2}\sum_{i,j} V(r_{ij}) + \sum_{i} F(\bar{\rho}_i) \quad (1)$$

where V is a pair potential as a function of distance r_{ij} between atoms i and j, and F is the embedding energy as a function of the

Table 1
Simulation parameters.

	No. 1	No. 2	No. 3	No. 4	No. 5
Relaxing time (ps)			50		
Discharge duration (ps)			4.8		
Power density (GW/cm^2)	2.447	1.718	1.468	1.004	0.781
Discharge column temperature (K)			7000		
Discharge column radius (Å)			30		
Total calculation time (ps)	83.6	83.6	80	78	78

host electron density $\bar{\rho}_i$ induced at site i by all other atoms in the system.

2.4. Heat transfer

In metals, heat is transferred by both the lattice vibration and thermal movement of free electrons. Since conventional MD methods are able to consider only heat conduction by lattice vibration, many researchers have attempted to modify the MD calculation to compensate for the influence of free electrons in metals [5,14,15]. However, theoretically acceptable methods have yet to be developed. Therefore in this study, the action of free electrons was neglected, and only the forming process of discharge craters and gap phenomena due to heat transfer by lattice vibration were studied. Although some of the simulation results did not agree with experimental ones quantitatively, conclusions obtained from the simulation in this paper provide some useful explanations for understanding the material removal mechanism and the gap phenomena in EDM.

3. Material removal mechanism

The material removal process and forming process of discharge craters were simulated using the parameters shown in Table 1. Although the spatiotemporal scale of the model used in this simulation is significantly small compared with those in actual EDM, the simulation results will be useful enough for qualitative understanding of the gap phenomena described in Section 1. Moreover, with the rapid advancement of the pulse generator, the minimum attainable discharge energy will be decreased further, realizing nano-EDM where quantitative comparison between the MD simulation and practical results will be possible.

The simulation program was run on a personal computer installed with a four-core CPU whose clock was 2.33 GHz and two 2 GB DDR2 667 SDRAM whose clock was 166 MHz. This program had a parallel structure based on MPI (Message Passing Interface), and MPICH. nt. 1.2.5 was used to implement MPI. The typical duration of one simulation was about 15 h.

Fig. 4 shows the simulation results of the material removal process of an electrode using the parameters No. 1 shown in Table 1. Thermal energy input into the electrode raises the temperature at the discharge spot and changes the temperature distribution in the electrode. When the temperature rises over the melting point (1358 K)/evaporating point (2840 K), the material will melt/vaporize. As shown in Fig. 4, when discharge just ends at 4.8 ps, the material on and near the electrode surface melts and even vaporizes in the top area. The vaporized material then begins departing from the electrode surface mostly in the form of single atom. Material is also vaporized at the electrode beneath the free surface, forming small bubbles as seen at 6 ps. Because the melting and vaporization occur in a very short time period and in a very narrow space, the pressure of the melted and vaporized material becomes extremely high, resulting in the rapid expansion of bubbles. When the border of a bubble reaches the electrode surface at 8.4 ps, the pressure difference between the bubble and vacuum results in the explosion of this bubble. This kind of explosion removes the molten material from the electrode surface mostly in the form of clusters. Consequently, the material removal mechanism in EDM can be explained in two ways: one by vaporization and the other by the explosion of bubbles generated in the material. These results indicate that removal can occur without the help of dielectric liquid [16].

Fig. 5 shows the calculated temperature distribution expressed by the gray scale in the middle section of the electrode at the end of the discharge duration using the parameters No. 3 shown in Table 1. D is the diameter of the discharge column. The part on the dotted line in Fig. 5 can be considered the melted pool. It was found that the diameter of this melted pool is larger than that of the discharge column. Fig. 6 shows the calculated temperature distribution 75.2 ps after the end of discharge. By comparing the melted pool in Fig. 5 with the shape of the discharge crater in Fig. 6, it can be seen that only a small part of the melted pool is removed and the remaining part is resolidified. This result agrees with the results reported by Van Dijck [17] who found experimentally that the metal removal

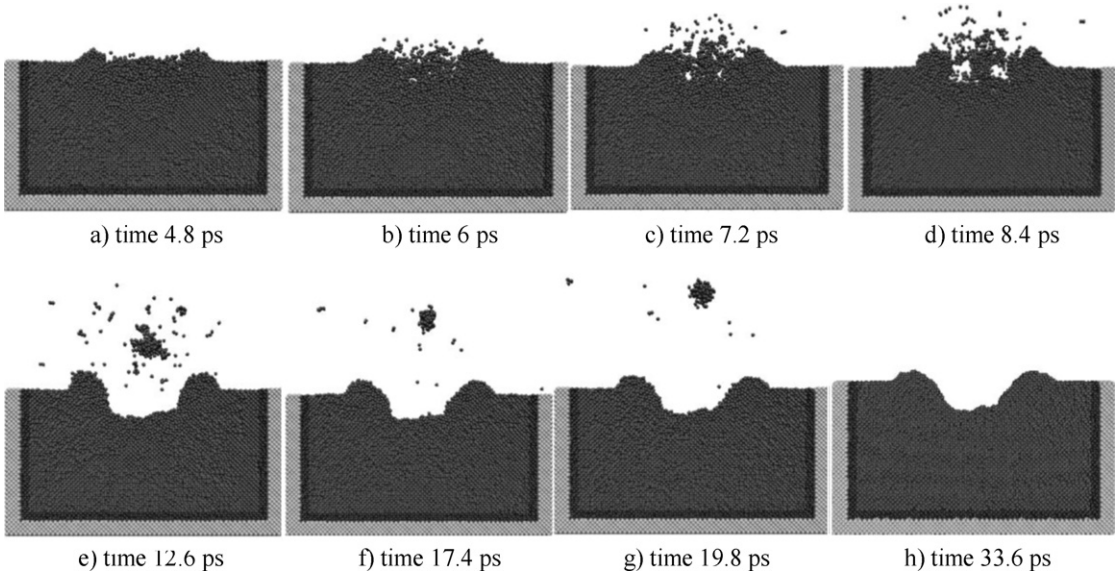

Fig. 4. Material removal process of electrode.

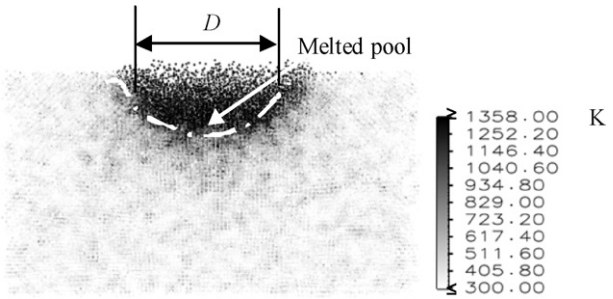

Fig. 5. Temperature distribution in middle section of electrode at end of discharge duration with power density of 1.468 GW/cm^2.

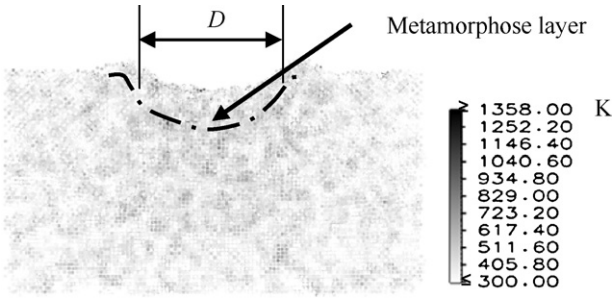

Fig. 6. Temperature distribution in middle section of electrode at 25.2 ps after end of discharge with power density of 1.468 GW/cm^2.

efficiency, defined as the ratio of the ejected to melted volume, was 0.01–0.1.

4. Influence of power density on removal process

4.1. Influence on volume of removed atoms

Fig. 7 shows electrode atoms in the discharge gap 12 ps after dielectric breakdown under different power densities. It can be confirmed that the cluster size becomes smaller as the power density decreases. From this, it can be concluded that when the power density is higher, bubble explosion due to superheating [17] plays the primary role in the removal process, and the material is removed mostly in the form of clusters. When the power density is lower, vaporization plays the primary role in the removal process, and the material is removed mostly in the form of single atoms.

4.2. Influence on metal removal efficiency

The metal removal efficiency, defined by Van Dijck [17] as the ratio of the ejected to melted volume, was investigated. Influences of power density on the diameter and depth of the melted area and the metal removal efficiency are shown in Fig. 8. It was found that higher power densities result in larger diameter and depth of the melted area as well as higher metal removal efficiency. The metal

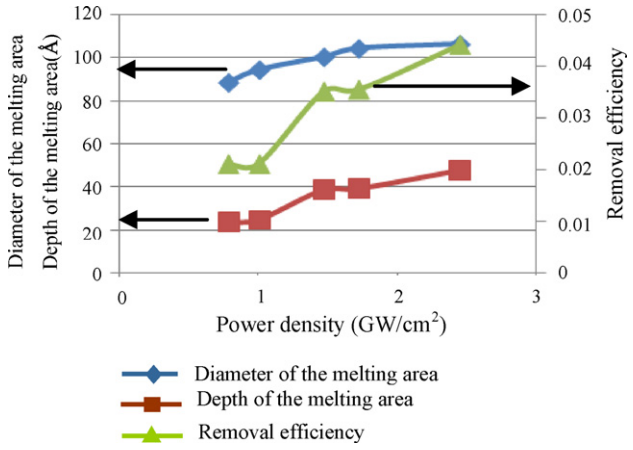

Fig. 8. Influence of power density on diameter and depth of melting area and metal removal efficiency.

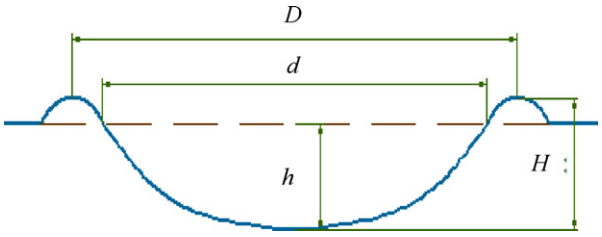

Fig. 9. Definition of discharge crater shape.

removal efficiencies obtained in the present work coincide with those obtained experimentally by Van Dijck [17]. As presented in Fig. 8, the change in the metal removal efficiency is similar to that in the depth of the melted area, indicating that the depth of the melted area has more significant effects on the metal removal efficiency.

4.3. Influence on shape characteristics of discharge crater

As shown in Fig. 9, the discharge crater shape was characterized by the parameters: removal diameter d, removal depth h, diameter of discharge crater D, and depth of discharge crater H. Influences of the power density on the shape parameters of discharge craters are shown in Fig. 10. It was found that all the shape parameters increase with increasing power density.

5. Forming mechanism of bulge around discharge crater

It is well known that a bulge is usually formed around a discharge crater. Since the bulge affects the roughness of the machined surface and the discharge location, researches on the forming mechanism of the bulge are beneficial for improving the machining properties of micro EDM.

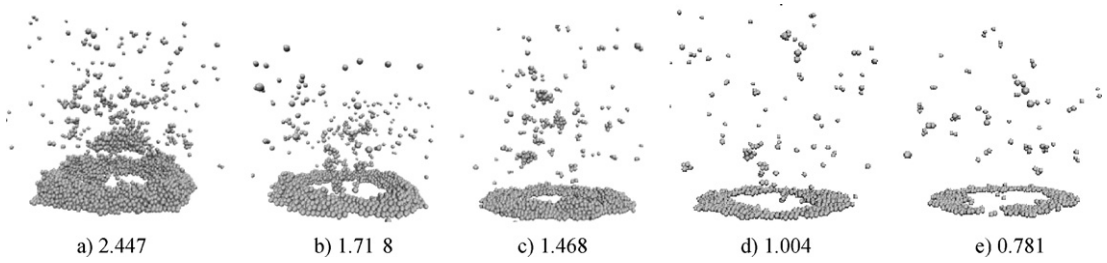

Fig. 7. Electrode atoms in discharge gap with increasing power density from 0.781 to 2.447 GW/cm^2 at 12 ps after dielectric breakdown.

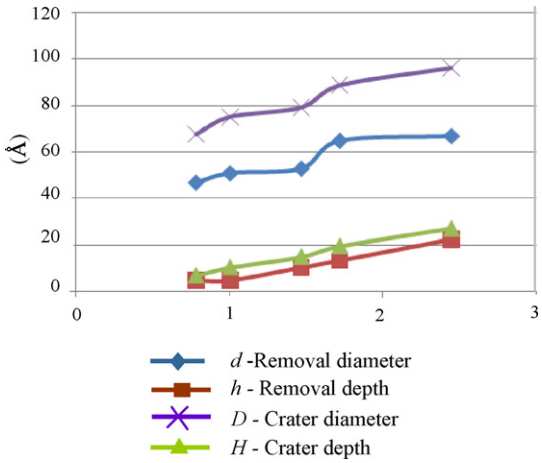

Fig. 10. Relation between shape parameters of discharge crater and power density.

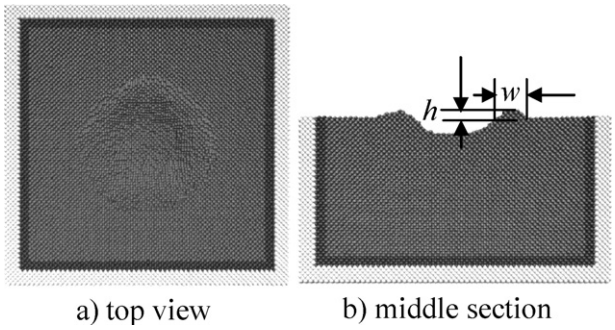

Fig. 11. Bulge around discharge crater generated on electrode at 30 ps after dielectric breakdown with power density of 1.468 GW/cm^2.

Fig. 11 shows the simulation results of the discharge crater of the electrode at 30 ps after dielectric breakdown with the power density of 1.468 GW/cm^2. It was found that a bulge of about 1.5a in height and 4.5a in width was formed around the discharge column. These simulation results show that there are two kinds of mechanisms affecting bulge formation. The first is that the extremely high pressure generated in the workpiece beneath the discharge column creates a significantly large pressure gradient in the melted pool in the radial direction, resulting in the acceleration of atoms not only in the direction normal to the surface but also in the directions tangential to the periphery of the crater. Thus the melted material is ejected from the center of the discharge column and protrudes into the gap space, forming the bulge around the crater. Fig. 12 shows the calculation results of the displacement of atoms. The displacement of atoms between the dotted lines indicates the shear flow of the molten material caused by the pressure gradient. The second mechanism is that a part of the ejected material accumulates on the

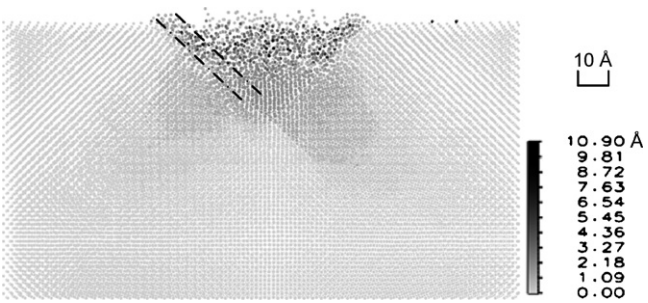

Fig. 12. Displacement of atoms in cross section of electrode at 3.6 ps.

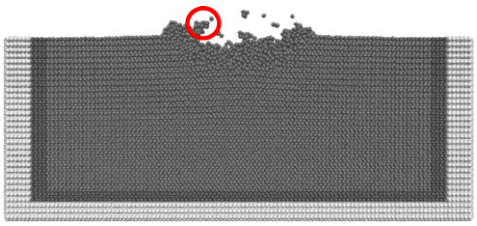

Fig. 13. Cross section of electrode at 8.4 ps after dielectric breakdown.

Table 2
Simulation parameters.

Pore diameter (Å)	20
Relaxing time (ps)	50
Discharge duration (ps)	5.4
Power density (GW/cm^2)	2.535
Discharge column temperature (K)	7000
Discharge column radius (Å)	35
Total calculation time (ps)	90

bulge formed due to the first forming mechanism. Fig. 13 shows a large cluster ejected from the melted pool sticking to the bulge.

6. Influences of micro pores in electrode material on discharge crater

There are various unavoidable defects in the electrode material, like micro cracks, pores, impurities, etc. which may exert certain influences on machining quality in micro-machining. Thus, the influences of micro pores preexisting in the electrode material on the forming process of discharge craters were investigated in this study.

Table 2 shows simulation parameters for a spherical pore with a diameter of 2 nm. Fig. 14 shows the pore positions, in which the dotted lines represent the boundaries of the discharge crater and melted area, respectively, obtained with the simulation parameters shown in Table 2 when no pores exist in the electrode material. Simulation was carried out to study the influences on the forming process when pores are located at different positions near the two boundaries. Pore No. 1 is located on the sidewall of the discharge crater; No. 2 is located in the discharge crater; No. 3 is located just on the bottom boundary of the discharge crater; No. 4 is located in the melted area; and No. 5 is located just on the bottom boundary of the melted area. Table 3 shows simulation results comparing crater dimensions with pores and those without pore. It can be concluded that the diameter of the discharge crater slightly increases when pore exists, whereas the depth of the discharge crater and melted area increase conspicuously, resulting in higher machining surface roughness. It was also found that the depth of the discharge crater is influenced most significantly by pore No. 3 which is located at the

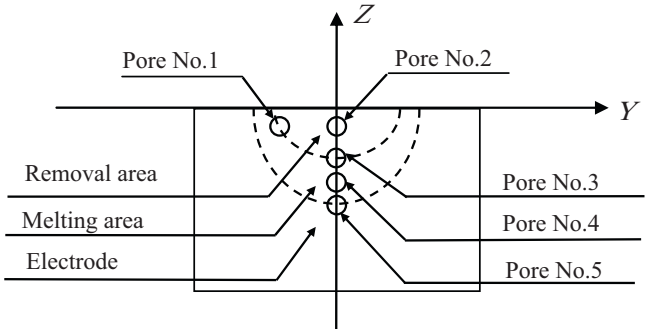

Fig. 14. Location of pores used in simulation.

Table 3
Influences of pore positions.

	No. 1	No. 2	No. 3	No. 4	No. 5	No pore
Crater diameter (nm)	10.5	10.6	10.5	10.6	10.5	10.4
Crater depth (nm)	3.65	3.90	4.20	3.95	3.95	3.60
Depth of melting area (nm)	5.6	5.6	5.7	5.8	5.8	5.3

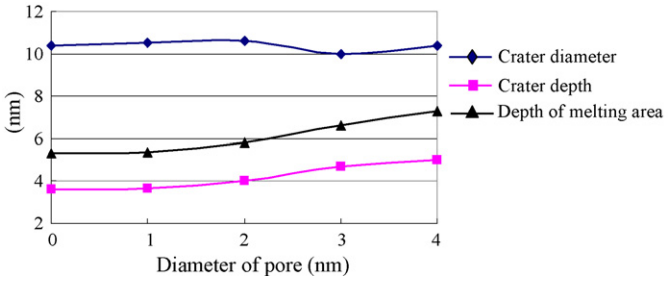

Fig. 15. Influences of pore diameters.

bottom of the discharge crater which is formed when there is no pore. When liquid boils, a bubble can only grow under the condition that the pressure inside the bubble is high enough to overcome the surface tension which works to collapse the bubble. Therefore, the existence of the nucleation centers promotes nucleate boiling [18]. Thus, it can be assumed that the explosion of bubbles occurs more easily when pores preexist prior to discharge inside the material, which leads to the increase in crater dimensions.

The influence of pore diameters on crater dimensions was studied under the conditions shown in Table 2 when the pore is located at No. 4 position. Simulation results shown in Fig. 15 indicate that as the diameter of the pore increases, the depths of the discharge crater and melted area increase, whereas no conspicuous change in the diameter of the discharge crater was observed. Fig. 16 shows the influence of a pore on the discharge crater, when the pore is 3 nm in diameter and located at the No. 4 position. The above results coincide with the actual EDM phenomena that the surface finish is affected by the impurities in the workpiece materials.

7. Distribution of removed materials in gap

The transfer of atoms between the anode and cathode across the gap due to discharge was simulated. In this simulation, the power density input into the anode and cathode was 1.693 GW/cm^2 and 1.227 GW/cm^2, respectively. The ratio of the former to the latter, about 1.38, was determined based on the fact that the energy distributed into the anode is greater than that into the cathode [19]. The distribution of ejected single atoms and clusters in the gap at different times is shown in Fig. 17. It was found that single atoms and clusters ejected from the electrodes move towards the opposite electrode. When clusters from different electrodes collide with each other, they break into smaller ones or single atoms followed by scattering. Along with this process, there are also some clusters or single atoms reaching the opposite electrode and settling there. The top views of the anode and cathode in Fig. 18 show that the number of anode atoms settled on the cathode surface are greater than that of cathode atoms settled on the anode surface. This is easy to explain using the conclusions obtained in Section 4.1. Since more thermal energy is distributed to the anode than to the cathode [19], clusters ejected from the anode are greater in number and larger than those from the cathode.

To show the distribution of the removed materials in the gap more clearly, only the atoms existing in the gap domain defined in Section 2.1 is presented in Fig. 19. In Fig. 19(a), there exist large clusters whose speed is relatively low. They are resolidified after reaching the free surfaces of the electrodes. There are also numerous small clusters scattered widely in the gap, forming small debris. Fig. 19(b) shows the atoms settled on the cathode surface. It was found that atoms of both the anode and cathode settle on the cath-

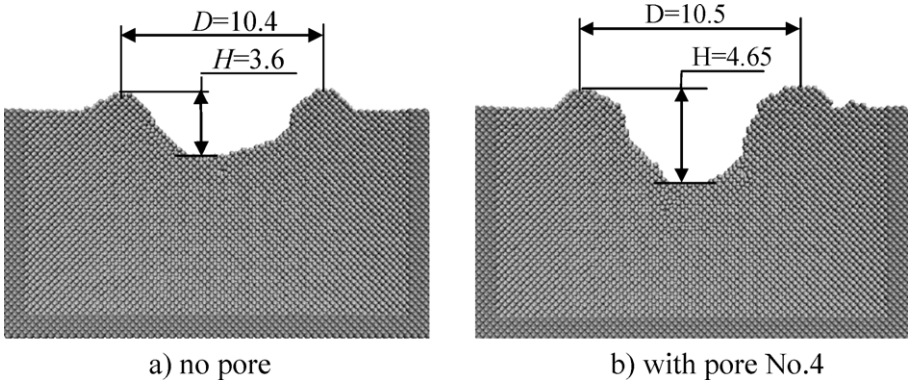

Fig. 16. Influences of micro pore on discharge crater.

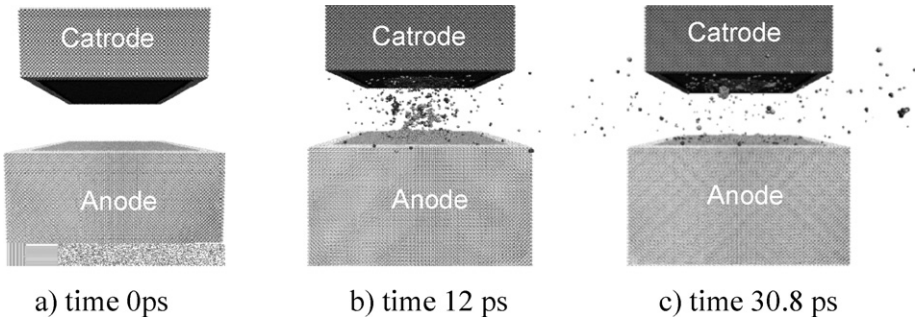

Fig. 17. Distribution of removed materials in gap at different time.

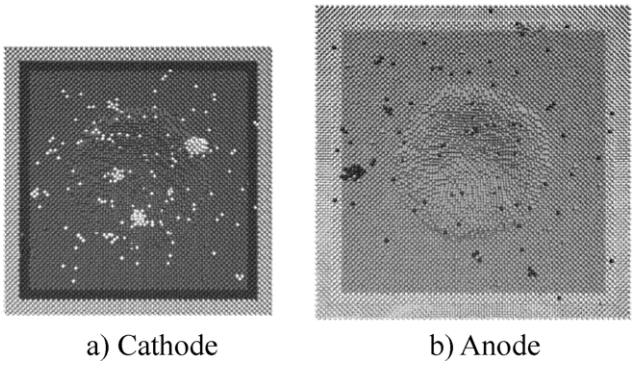

Fig. 18. Top views of anode and cathode at 30.8 ps.

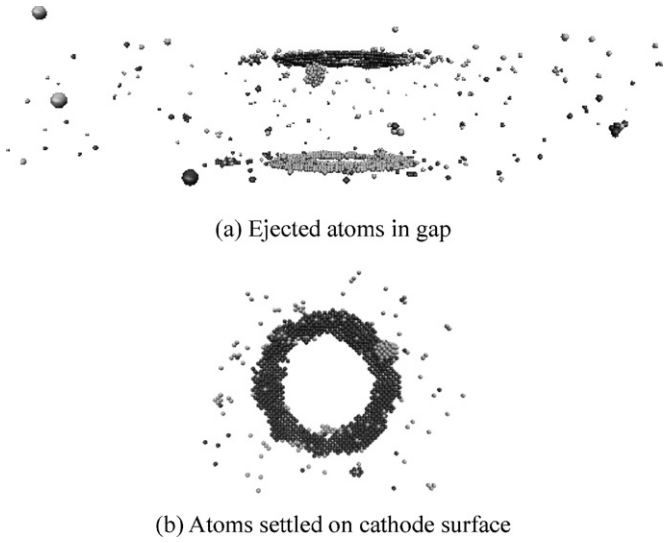

Fig. 19. Atoms existent in gap domain at 30.8 ps (dark and light particles show cathode and anode atoms, respectively.).

ode surface, indicating that a part of the removed material reaches the opposite electrode and settles there, and another part returns to the electrode from which it was ejected.

8. Conclusions

In this paper, the forming process of discharge craters in three dimensions was simulated, and material removal mechanism in EDM was analyzed using MD. The following conclusions were obtained:

- Material removal mechanism in EDM can be explained in two ways; one by vaporization and the other by the bubble explosion of superheated metals. When the power density is relatively low, vaporization plays the primary role and the material is removed mostly in the form of single atoms; when the power density is relatively high, bubble explosion plays the dominant role and the material is removed mostly in the form of clusters.
- The metal removal efficiency is 0.02–0.05, leaving most of the melted pool resolidified.
- As the power density increases, the diameter and depth of the melted area increase, as does the metal removal efficiency, suggesting increased machining efficiency.
- Bulge is formed due to two mechanisms. The first is that the extremely high pressure in the superheated material causes ejection of the melted material from the center of the discharge column and protrusion into the gap, forming the bulge around the crater. The second is that a part of the ejected material accumulates on the bulge formed by the first forming mechanism.
- When there are pores prior to the ejection of the electrode material, explosion of bubbles can occur much easily, resulting in the increased depth of the discharge crater and melted area.
- The first part of the removed material becomes debris in the gap, the second part settles on the surface of the opposite electrode, and the last part returns to the surface of the electrode from which it was ejected.

Some of the above conclusions are already verified in the actual EDM processes. Although the spatiotemporal scale of the model used in this simulation is significantly small compared with those in actual EDM, the conclusions obtained above will be useful enough for understanding the EDM gap phenomena qualitatively.

Acknowledgements

This study was sponsored by the National Natural Science Foundation of China (General Program, 50775056) and the 111 Project (B07018).

References

[1] Hanaoka D, Yoshida M. Comparison of a crater by single pulse discharge in dry and in liquid. In: Proceedings of 2007 annual meeting of Japan Society of Electrical Machining Engineers. 2007. p. 293–6 [in Japanese].
[2] Araie I, Sano S, Kunieda M. Study of craters in micro electrical discharge machining. In: Proc. of spring meeting of JSPE in 2005. 2005. p. 1315–6 [in Japanese].
[3] Pittaway LG. Temperature distributions in thin foil and semi-infinite targets bombarded by an electron beam. Brit J Appl Phys 1964;15:967–82.
[4] Saito N, Kobayashi K. Machining principle and characteristics of electric discharge machining. Mitsubishi Denki Giho 1967;41(10):1222–30 [in Japanese].
[5] Shimada S, Ikawa N, Ohmori G, Tanaka H, Uchikoshi J. Molecular dynamics analysis as compared with experimental results of micromachining. Ann CIRP 1992;41(1):117–20.
[6] Shimada S, Ikawa N, Tanaka H, Ohmori G, Uchikoshi J, Yoshinaga H. Feasibility study on ultimate accuracy in microcutting using molecular dynamics simulation. Ann CIRP 1993;42(1):91–4.
[7] Ohmura E, Fukumoto I. Study on thermal shock phenomena due to laser irradiation using molecular dynamics. Int J JSPE 1995;29(2):148–50.
[8] Kalyanasundaram V, Virwani KR, Spearot DE, Malshe AP, Rajurkar KP. Understanding behavior of machining interface and dielectric molecular medium in nanoscale electro-machining. Ann CIRP 2008;57(1):199–202.
[9] Shimada S, Tanaka H, Mohri N, Takezawa H, Ito Y, Tanabe R. Molecular dynamics analysis of self-sharpening phenomenon of thin electrode in single discharge. J Mater Process Technol 2004;149:358–62.
[10] Cui JZ. Research on foundational law of micro-EDM and its simulation. Dissertation for the Doctoral Degree of Harbin Institute of Technology; 2007. p. 85–96 [in Chinese].
[11] Takeuchi H, Kunieda M. Effects of volume fraction of bubbles in discharge gap. In: Proc. of ISEM XV. 2007. p. 63–8.
[12] Natsu W, Ojima S, Kobayashi T, Kunieda M. Temperature distribution measurement in EDM Arc plasma using spectroscopy. JSME Int J C 2004;47(1):384–90.
[13] Mishin Y, Mehl MJ, Papaconstantopoulos DA, Voter AF, Kress JD. Structural stability and lattice defects in copper: ab initio, tight-binding, and embedded-atom calculations. Phys Rev B 2001;63(22):224106.
[14] Ohmura E, Fukumoto I. Modified molecular dynamics simulation on laser ablation of metal. Int J JSPE 1997;31(3):206–10.
[15] Hayama T, Tsuji T. Surface processing analysis by molecular dynamics with consideration of the movement of free electrons. In: The 55th National Congress of Theoretical and Applied Mechanics, vol. 55. 2006. p. 202–3 [in Japanese].
[16] Yoshida M, Kunieda M. Study on the distribution of scattered debris generated by a single pulse discharge in EDM process. IJEM 1998;3:39–47.
[17] Van Dijck F. Physico-mathematical analysis of the electro discharge machining process. Dissertation of Katholieke Universiteit Leuven; 1973.
[18] Holman JP. Hest transfer. 9th ed. New York: McGraw Hill Book Company; 2002.
[19] Xia H, Kunieda M, Nishiwaki N. Removal amount difference between anode and cathode in EDM process. IJEM 1996;1:45–52.